

# Magnetic properties of amorphous $\text{Co}_x\text{Nb}_{100-x}$ alloys produced by mechanical alloying

K. D. Machado \*, R. C. da Silva, J. C. de Lima, T. A. Grandi,  
A. A. M. Gasperini, C. E. M. Campos

*Depto de Física, Universidade Federal de Santa Catarina, Trindade, Cx. P. 476,  
88040-900, Florianópolis, Santa Catarina, Brazil*

---

## Abstract

Three amorphous  $\text{Co}_x\text{Nb}_{100-x}$  alloys,  $\text{Co}_{25}\text{Nb}_{75}$ ,  $\text{Co}_{57}\text{Nb}_{43}$  and  $\text{Co}_{80}\text{Nb}_{20}$ , were produced by Mechanical Alloying starting from the elemental powders. Their magnetic properties were determined using an alternating gradient force magnetometer (AGFM), and the remanent magnetizations, saturation fields and coercive fields were obtained from the hysteresis loop. The alloys have a relatively high saturation field, which decreases as the composition becomes richer in Co. The coercivity and remanent magnetization reach an optimal value around 57% at.Co, making  $a\text{-Co}_{57}\text{Nb}_{43}$  the hardest magnetic material among the three alloys. Further addition of Co produces a soft alloy.

*Key words:* Mechanical alloying, magnetic amorphous alloys

*PACS:* 61.43.Dq, 75.50.Kj, 81.20.Ev

---

## 1 Introduction

Mechanical alloying (MA) technique [1] is an efficient means for synthesizing crystalline compounds, amorphous alloys and unstable and metastable phases [2,3,4,5,6,7,8]. MA has also been used to produce materials with nanometer sized grains and alloys whose components have large differences in their melting temperatures and are thus difficult to produce using techniques based on melting. It is a dry milling process in which a metallic or non-metallic powder mixture is actively deformed in a controlled atmosphere under a highly

---

\* Corresponding author.

*Email address:* kleber@fisica.ufsc.br (K. D. Machado).

energetic ball charge. The few thermodynamics restrictions on the alloy composition open up a wide range of possibilities for property combinations [9], even for immiscible elements [10]. The temperatures reached in MA are very low, and thus this low temperature process reduces reaction kinetics, allowing the production of poorly crystallized or amorphous materials.

Co–Nb is one of many systems of interest due to their superior magnetic properties [11]. Its equilibrium phase diagram shows three stable phases  $\text{Co}_7\text{Nb}_6$ ,  $\alpha\text{-Co}_2\text{Nb}$  and  $\text{Co}_3\text{Nb}$ , and at least one high-temperature alloy,  $\beta\text{-Co}_2\text{Nb}$  [12]. Besides the techniques used to produce Co–Nb alloys, which are described in Ref. [12], Co–Nb amorphous films have been formed by ion-beam mixing (IM) of multilayer films [11]. The amorphization range is determined to vary from 23 to 80 at.% Co. Zeng *et al.* [11] have also shown that induced growth of such amorphous films can be performed by the ion beam assisted deposition (IBAD) technique. Here, we have used MA to produce amorphous  $\text{Co}_x\text{Nb}_{100-x}$  alloys starting from the crystalline elemental powders. The chosen compositions were  $\text{Co}_{25}\text{Nb}_{75}$  ( $\alpha\text{-Co}_{25}\text{Nb}_{75}$ ),  $\text{Co}_{57}\text{Nb}_{43}$  ( $\alpha\text{-Co}_{57}\text{Nb}_{43}$ ) and  $\text{Co}_{80}\text{Nb}_{20}$  ( $\alpha\text{-Co}_{80}\text{Nb}_{20}$ ). Their magnetic properties were determined using an alternating gradient force magnetometer (AGFM), and the remanent magnetizations, saturation fields and coercive fields were obtained from the hysteresis loop. The alloys have a relatively high saturation field, which decreases as the composition becomes richer in Co. The coercivity and remanent magnetization reach an optimal value around 57% at.Co, making  $\alpha\text{-Co}_{25}\text{Nb}_{75}$  the hardest magnetic material among the three alloys. If the amount of Co is even increased, the alloy becomes a soft magnetic material.

## 2 Experimental Procedures

Binary mixtures of Co and Nb crystalline elemental metals powders, with nominal composition  $\text{Co}_{25}\text{Nb}_{75}$ ,  $\text{Co}_{57}\text{Nb}_{43}$  and  $\text{Co}_{80}\text{Nb}_{20}$  were sealed together with several steel balls, under argon atmosphere, in steel vials. The weight ratio of the ball to powder was 6:1 for all compositions. The vials were mounted in a Spex 8000 shaker mill and the samples were milled for 40 h. In order to keep the vial temperature close to room temperature, a ventilation system was used. The compositions of the as-milled alloys were determined by X-ray fluorescence method using an EDX-700 Shimadzu equipment, giving a composition of 25 at.%Co and 75 at.%Nb for the first alloy, 57 at.%Co and 43 at.%Nb for the second, and 79 at.%Co and 21 at.%Nb for the third. Impurity traces were not detected. The hysteresis loops were obtained at room temperature using a home-made alternating gradient force magnetometer by applying the magnetic field, up to  $\pm 5.0$  kOe, parallel to the plane of sample.

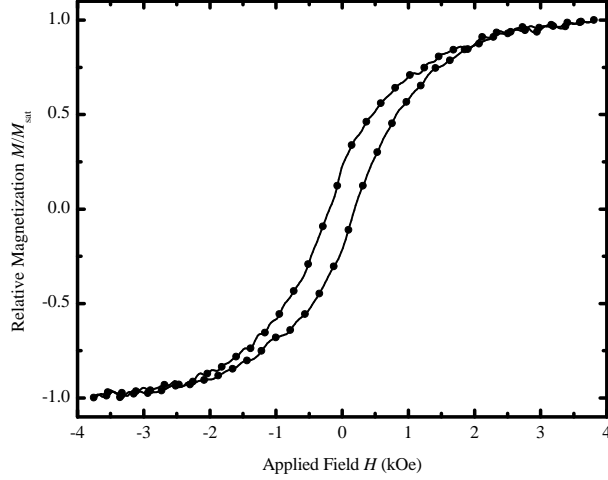


Fig. 1. Hysteresis loop of  $a\text{-Co}_{25}\text{Nb}_{75}$ .

### 3 Results and Discussion

The hysteresis loop of  $a\text{-Co}_{25}\text{Nb}_{75}$  showing the relative magnetization  $M/M_{\text{sat}}$  as a function of the applied field  $H$  can be seen in fig. 1. From this figure, we found the remanent magnetization  $M_{\text{rem}}$ , which is about 22% of the saturation value ( $M_{\text{sat}}$ ), and the saturation ( $H_s$ ) and coercive ( $H_c$ ) fields are  $H_s = 3809$  Oe and  $H_c = 183$  Oe, respectively.

Figure 2 shows the hysteresis loop of  $a\text{-Co}_{57}\text{Nb}_{43}$ . From this figure it can be seen a reduction in the saturation field, which is now  $H_s = 2144$  Oe, and an increase both in coercivity ( $H_c = 254$  Oe) and in remanent magnetization, which is 33% of the saturation value for this alloy.

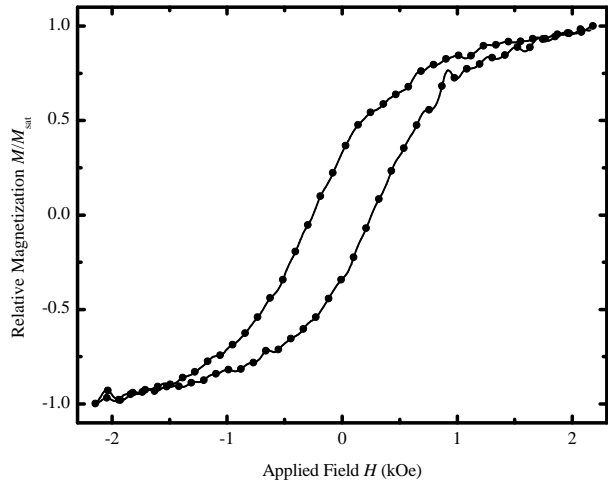


Fig. 2. Hysteresis loop of  $a\text{-Co}_{57}\text{Nb}_{43}$ .

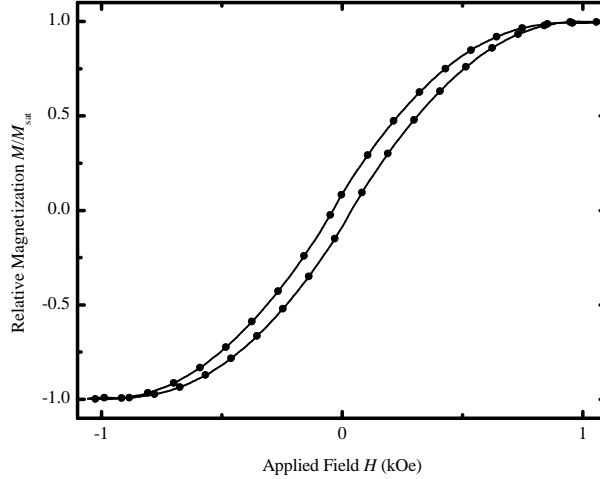
The hysteresis loop of the third alloy,  $a\text{-Co}_{80}\text{Nb}_{20}$ , is seen in fig. 3. From this figure, we found  $H_s = 1058$  Oe for the saturation field, which shows again a re-

Table 1

Magnetic parameters obtained for amorphous  $\text{Co}_x\text{Nb}_{100-x}$  alloys.

$x$ (% at.Co)	$H_s$ (Oe)	$H_c$ (Oe)	$M_{\text{rem}}/M_{\text{sat}}$ (%)
25	3809	183	22
57	2144	254	33
80	1058	35	8

duction when compared with the values found for  $a\text{-Co}_{25}\text{Nb}_{75}$  and  $a\text{-Co}_{57}\text{Nb}_{43}$ , but its coercivity decreases to  $H_c = 35$  Oe and only 8% of the magnetization is retained from its saturation value. Although the addition of Co to the  $a\text{-Co}_{25}\text{Nb}_{75}$  alloy has produced a harder magnetic material, the increase in the magnetic properties seems to reach an optimal value around 57%at.Co. After that, the amorphous  $\text{Co}_x\text{Nb}_{100-x}$  alloys become a softer magnetic material, as shown by the data found for  $a\text{-Co}_{80}\text{Nb}_{20}$ . Table 1 shows the data obtained for the three alloys.

Fig. 3. Hysteresis loop of  $a\text{-Co}_{80}\text{Nb}_{20}$ .

## 4 Conclusion

Amorphous  $\text{Co}_x\text{Nb}_{100-x}$  alloys were prepared by MA and their magnetic properties investigated. The main conclusions of this study are:

- (1) Formation of  $a\text{-Co}_x\text{Nb}_{100-x}$  by MA in the range  $25 \leq x \leq 80$  was confirmed experimentally.
- (2) Amorphous  $\text{Co}_x\text{Nb}_{100-x}$  alloys are magnetic materials, showing relatively high saturation fields, which decreases as the alloy composition becomes richer in Co.
- (3) Coercivity and remanent magnetization increase when composition goes from 25% at.Co to 57% at.Co, making the  $a\text{-Co}_{57}\text{Nb}_{43}$  the hardest mag-

netic material among the three alloys. However, further increase in the amount of Co atoms did not produce a harder magnetic alloy.  $H_c$  and  $M_{rem}$  decrease and  $a\text{-Co}_{80}\text{Nb}_{20}$  becomes the softest alloy.

## Acknowledgements

We thank the Brazilian agencies CAPES and CNPq for financial support.

## References

- [1] C. Suryanarayana, Prog. Mater. Sci. 46 (2001) 1.
- [2] J. C. de Lima, K. D. Machado, V. Drago, T. A. Grandi, C. E. M. Campos, D. M. Trichês, J. Non-Cryst Solids 318 (2003) 121.
- [3] A. W. Weeber, H. Bakker, Physica B 153 (1988) 93.
- [4] D. K. Mukhopadhyay, C. Suryanarayana, F. H. Froes, Scripta Metall. Mater. 30 (1994) 133.
- [5] A. R. Yavari, P. J. Desré, T. Benameur, Phys. Rev. Lett. 68 (1992) 2235.
- [6] K. D. Machado, J. C. de Lima, C. E. M. Campos, T. Grandi, A. A. M. Gasperini, Sol. State. Commun. 127 (2003) 477.
- [7] K. D. Machado, J. C. de Lima, C. E. M. de Campos, T. A. Grandi, D. M. Trichês, Phys. Rev. B 66 (2002) 094205.
- [8] C. E. M. Campos, J. C. de Lima, T. A. Grandi, K. D. Machado, P. S. Pizani, Physica B 324 (2002) 409.
- [9] J. M. Poole, J. J. Fischer, Mater. Technol. 9 (1994) 21.
- [10] M. Abbate, W. H. Schreiner, T. A. Grandi, J. C. de Lima, J. Phys.: Cond. Matter 13 (2001) 5723.
- [11] F. Zeng, F. Pan, J. Alloy Comp. 335 (2002) 181.
- [12] T. B. Massalki, Binary alloys phase diagram, ASM Publ., 1990.